Reflection-type electromagnetically induced transparency analogue in terahertz metamaterials*

Ding Chun-Feng(丁春峰)[a)b)c)], Zhang Ya-Ting(张雅婷)[a)b)], Yao Jian-Quan(姚建铨)[a)b)†], Sun Chong-Ling(孙崇玲)[d)], Xu De-Gang(徐德刚)[a)b)], and Zhang Gui-Zhong(张贵忠)[a)b)]

[a)] College of Precision Instrument and Opto-electronics Engineering, Institute of Laser and Opto-electronics, Tianjin University, Tianjin 300072, China

[b)] Key Laboratory of Opto-electronics Information Technology, Tianjin University, Tianjin 300072, China

[c)] Henan Key Laboratory of Laser and Opto-electric Information Technology, Zhenzhou 450052, China

[d)] State Key Laboratory of Precision Measuring Technology and Instruments, Tianjin University, Tianjin 300072, China

(Received 14 April 2014; revised manuscript received 26 May 2014; published online 10 October 2014)

A reflection-type electromagnetically induced transparency (EIT) metamaterial is proposed, which is composed of a dielectric spacer sandwiched with metallic patterns and metallic plane. Experimental results of THz time domain spectrum (THz-TDS) exhibit a typical reflection of EIT at 0.865 THz, which are in excellent agreement with the full-wave simulations. A multi-reflection theory is adopted to analyze the physical mechanism of the reflection-type EIT, showing that the reflection-type EIT is a superposition of multiple reflection of the transmission EIT. Such a reflection-type EIT provides many applications based on the EIT effect, such as slow light devices and nonlinear elements.

Keywords: electromagnetically induced transparency (EIT), metamaterial, multiple-reflection interference

PACS: 42.50.Gy, 78.67.Pt, 42.25.Hz **DOI:** 10.1088/1674-1056/23/12/124203

1. Introduction

Electromagnetically induced transparency (EIT) which can improve the dispersion properties of the medium and inhibit the absorption of medium, is a quantum interference phenomenon occurring in the medium where two laser beams with different transitions act on it.[1] Recently, using metamaterials to realize the quantum phenomenon of EIT has aroused great interest. Many researchers have proposed different structures of metamaterials by mainly using split-ring resonators (SRRs), cut wires (CWs), and plasmonic waveguides to realize the EIT effect.[2–14] Following appropriate design rules,[3,4,7,15–20] the prominent EIT phenomenon could be realized in metamaterials by destructive interference between different resonance modes. There are two common methods to manipulate the resonance modes by rationally designing the structure of metamaterials. The first method is to design two substructures in the metamaterials which act as bright mode and dark mode, respectively.[3–7] The incident light is only coupled to the bright mode, but not directly coupled to the dark mode. It is the coupling between the dark mode and the bright mode that leads to the EIT. The second method is to design two substructures, known as super-radiant (low quality factor) and sub-radiant (high quality factor) resonators, both of which can be directly excited by the incident light. In this case, the EIT can be realized through properly controlling the coupling of the two resonators.[8–10]

In most previously designed EIT metamaterials, the characteristics of the EIT were usually demonstrated through the transmission spectrum.[3–20] However, the reflection of EIT, an important physical component the same as the transmission of the EIT, is ignored. In this work, a reflection-type EIT metamaterial functioning in the terahertz (THz) regime is proposed, fabricated, and characterized, which is composed of a dielectric substrate sandwiched with metallic patterns and metallic planes. In the designed metamaterials, we find two different metal patterns on the top layer which act as bright and dark resonators, respectively, leading to the EIT, then the EIT spectrum is multi-reflected between the top metallic structure and the ground plane. The complex amplitudes of all reflected waves from the air/metallic layer interface are then superposed.

2. Experiment

The unit structure is shown in Fig. 1(a). From top to bottom, the parts of the sandwiched structure are the metallic pattern, polyimide, and metallic plane, respectively. The metallic pattern consists of a CW and two SRRs, and both the metallic pattern and metallic plane are 0.2-μm-thick gold. The geometrical parameters are chosen to be $P_x = 80$, $P_y = 120$, $L = 102$, $l = 42$, $D_y = 20$, $s = 9$, $h = 8.5$, and $w = 5$ μm. The fabrication process of the sample is discussed as follows. Firstly, a 0.2-μm-thick gold film was thermally evaporated on a silicon substrate (n-type, 640 μm). Then, an 8.5-μm-thick polyimide layer was added to the gold film to form the spacer layer.

*Project supported by the National Natural Science Foundation of China (Grant Nos. 61205096 and 61271066).

†Corresponding author. E-mail: jqyao@tju.edu.cn

© 2014 Chinese Physical Society and IOP Publishing Ltd

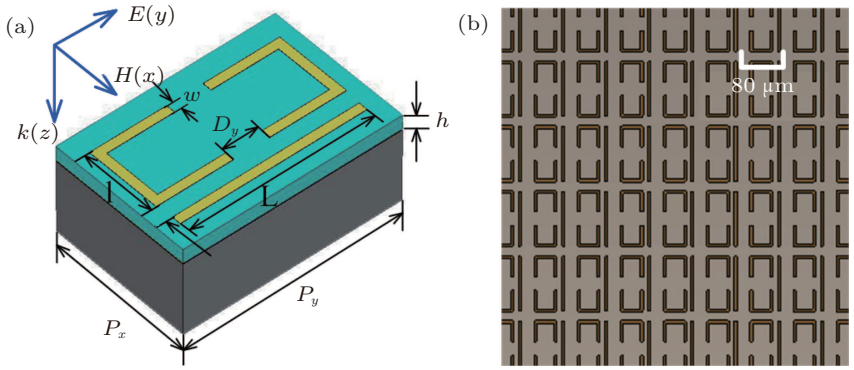


Fig. 1. (color online) (a) Schematic diagram of the unit structure. (b) Microscopic image of the fabricated metamaterials.

Finally, the 0.2-μm-thick gold patterns were fabricated by conventional optical lithography on the polyimide isolator. The total size of the sample is 18 mm×24 mm. Part of the microscope image of the fabricated structure is shown in Fig. 1(b).

The reflectance spectrum of the sample is measured using a terahertz time-domain spectroscopy (TDS). To normalize the reflectance spectrum, an unpatterned 0.2-μm-thick gold plane thermally evaporated on a silicon substrate is used as a reference of the sample. The normalized reflectance spectrum is defined as $|\tilde{R}| = |\tilde{E}_s(\omega)|/|\tilde{R}_r(\omega)|$, where $|\tilde{E}_s(\omega)|$ and $|\tilde{E}_r(\omega)|$ are the Fourier transform of the terahertz pulses reflected by the sample and the reference, respectively.

3. Results and discussion

To reveal the mechanism of the reflection-type EIT, we prepare three samples, i.e., the CW sample consisting of CW array, polyimide, and the gold plane, the SRR sample consisting of SRR arrays, polyimide, and the gold plane, and the reflection-type EIT sample consisting of CW, SRRs, polyimide, and the gold plane (see Fig. 1). When the polarization direction of the incident wave is parallel to the y orientation, the measured reflectance spectra are shown in Fig. 2, the CW sample shows a resonance at 0.865 THz. The SRR sample is inactive due to its symmetrical structure, though it supports an inductive–capacitive (LC) resonance at the same frequency. The reflection-type EIT sample shows a sharp reflection peak at 0.865 THz between two reflection valleys with the resonant frequencies of 0.811 THz and 0.924 THz, respectively. This form of reflectance spectrum is similar to that of the transmission spectrum of the EIT reported elsewhere.[15–20]

We carry out the full-wave numerical simulations to test the performances of the designed metamaterials using the CST Microwave Studio 2010. Here the gold electric conductivity is $\sigma = 4.561 \times 107$ s/m, and the dielectric constant of the polyimide is $\varepsilon = 3.1 \times (1 + 0.02\mathrm{i})$. The simulation conditions are as follows: the x and y directions are set as the periodic boundary conditions, and both the ports are perpendicular to the z direction and placed at the two surfaces of the sample, respectively. The electromagnetic waves with the y-polarized direction are normally incident upon the sample.

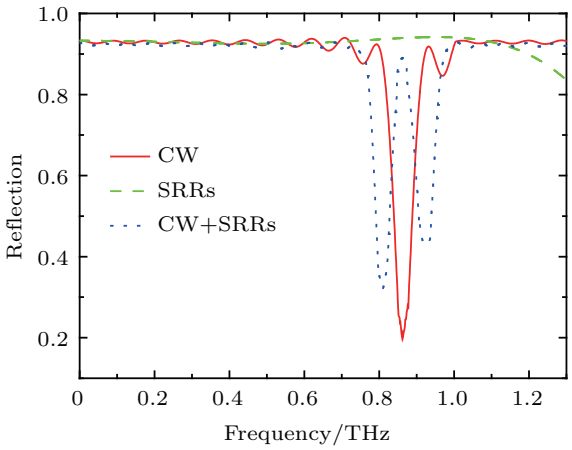


Fig. 2. (color online) Reflectance spectra of the three samples: (a) CW sample, (b) SRR sample, and (c) reflection-type EIT sample.

The two-dimensional (2D) distributions of the electric field at 0.865 THz for the three samples are shown in Fig. 3, where figure 3(a) indicates that the CW is strongly excited by the incident plane wave with a high electric field forming at its ends, figure 3(b) shows that there is hardly any induced electric field in the SRR sample due to the symmetry of the structure, and figure 3(c) displays that the LC resonance of the SRRs is

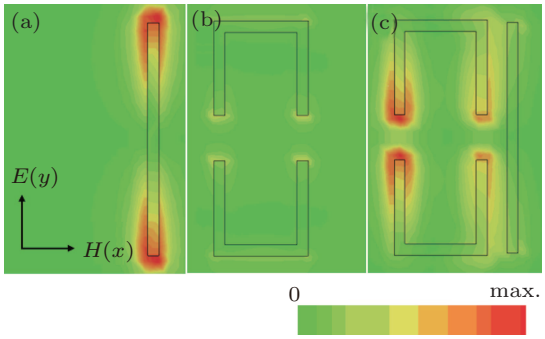


Fig. 3. (color online) Electric field distributions of (a) CW sample, (b) SRRs sample, and (c) reflection-type EIT sample.

excited by the CW resonance via near coupling. Therefore, in the reflection-type EIT sample, the CW and SRR serve as the bright and dark modes, respectively. The near field coupling between the two modes leads to a destructive interference, and as a consequence, there appears a sharp transparency peak in a broad absorption background.

The simulated spectrum of the reflection-type sample is also demonstrated in Fig. 4 (the thin solid line), showing that there is a resonant peak at 0.865 THz. Excellent agreement between simulation and experiment results except for a slight difference is observed. We believe that the fabrication and measurement errors may be responsible for the discrepancy.

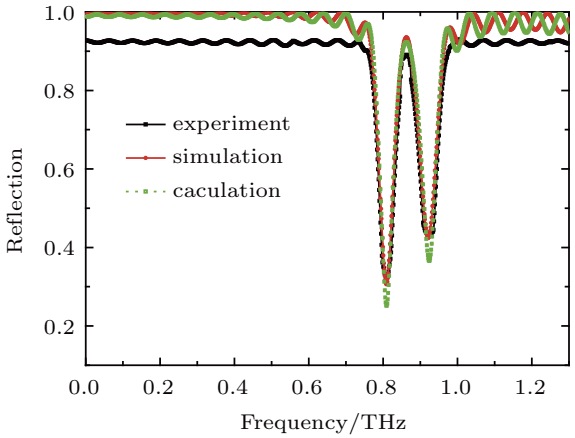


Fig. 4. (color online) Reflectance spectra acquired by experiment (the black line), simulation (the thin solid line), and calculation using multi-reflection theory.

To analyze the working mechanism of the designed structure, a transmittance EIT model is simulated for comparison. The structure of the transmittance EIT model is similar to the proposed structure shown in Fig. 1(a), except that the silicon wafer and metallic plane are removed. According to Ref. [16], this model is a representative structure which can lead to EIT when the dimensions of the CW and the SRRs are appropriately designed and the polarization direction of incident electromagnetic wave is parallel to the CW. In the transmittance EIT model, the CW acts as the bright resonator, while the SRRs act as the dark ones. The thin solid line (denoted by t) in Fig. 5(b) shows the simulated result. It is an ordinary EIT transmission spectrum, in which the amplitude and frequency of the resonance peak are different from the reflectance spectra shown in Fig. 4. We believe that it must be the metallic ground plane that is responsible for the discrepancies.

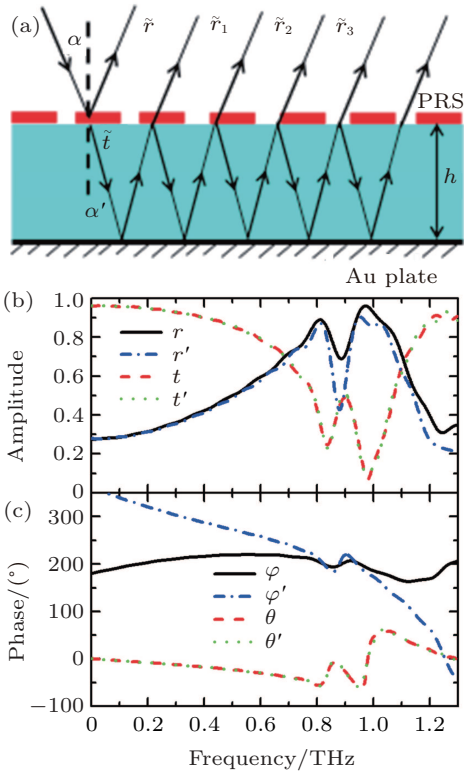


Fig. 5. (color online) (a) Fabry–Perot resonant model. Simulated (b) magnitudes and (c) phases of the reflection and transmission coefficients for the part reflection surface (PRS).

To gain a physical insight of the reflection-type EIT, we should quantitatively analyze the mechanisms of the designed metamaterials. Here we treat the reflectance EIT structure as a modified Fabry–Perot resonant model[20,21] to quantitatively analyze the reflectance spectrum. As demonstrated in Fig. 5(a), the metallic pattern represents a part reflection surface (PRS), and the gold plane represents a total reflection surface. When the electromagnetic wave at a certain angle is incident upon the PRS, part of the incident electromagnetic wave is reflected back with a reflection coefficient $\tilde{r} = r\mathrm{e}^{\mathrm{i}\varphi}$. At the same time, the rest transmits into the polyimide with a transmission coefficient $\tilde{t} = t\mathrm{e}^{\mathrm{i}\theta}$, then is reflected by the gold plane with a reflection coefficient $\tilde{r}'' = r''\mathrm{e}^{\mathrm{i}\pi}$. This part of electromagnetic wave is continually incident upon the dielectric/PRS interface, and divided into two plane waves. One is transmitted into air with a transmission coefficient $\tilde{t}' = t'\mathrm{e}^{\mathrm{i}\theta'}$, and the other is reflected back into the dielectric spacer with a reflection coefficient $\tilde{r}' = r'\mathrm{e}^{\mathrm{i}\varphi'}$. The multi-reflection process inside the spacer is illustrated in Fig. 3(a). The total reflection outside the PRS is a superposition of the multiple reflections:

$$\tilde{R} = \tilde{r} + \tilde{r}_1 + \tilde{r}_2 + \tilde{r}_3 + \cdots = \frac{r\mathrm{e}^{\mathrm{i}\varphi} - [rr'\mathrm{e}^{\mathrm{i}(\varphi+\varphi')} - tt'\mathrm{e}^{\mathrm{i}(\theta+\theta)'}]\exp\left[\mathrm{i}\left(-\dfrac{4\pi}{\lambda_0}\sqrt{\varepsilon}h\cos\alpha' + \pi\right)\right]}{1 + r'\exp\left[\mathrm{i}\left(\varphi + \pi - \dfrac{4\pi}{\lambda_0}\sqrt{\varepsilon}h\cos\alpha'\right)\right]}, \tag{1}$$

where $\delta = -(2\pi/\lambda_0)\sqrt{\varepsilon}2h\cos\alpha'$ is the phase difference of the reflected wave which differs from that of the preceding wave propagating in the dielectric spacer, and λ_0 is the wavelength in free space. Based on coefficients and phases of the reflection and transmission coefficients for the PRS as illustrated in Figs. 5(b) and 5(c), the total reflection is calculated from Eq. (1), and the result is shown in Fig. 4 (the dashed line), the calculated reflectance spectrum is in excellent agreement with results from both the full-wave simulation (the thin solid line) and the experiment (the thick line). This agreement verifies the rationality of using multi-reflection theory to analyze the performance of the EIT reflection, and importantly, this processing method enables us to understand the physical mechanism of the reflection-type EIT. When the THz beam is incident upon the metasurface with a polarization direction parallel to the CW, the CW can be directly excited by the incident electromagnetic wave, but the SRRs cannot. Because the resonant frequency of the CW is approximate to the SRR's, near-field coupling between the two different resonators will occur, then the SRR resonator is excited by the resonance of CW and leads to EIT. That is, the CW resonator provides the bright mode and the SRRs provide the dark mode in the process of EIT. Then, the transmittance spectrum of EIT is incident upon the spacer and is multi-reflected between the PRS and the ground plane. Finally, a destructive interference of multi-reflection beams results in the anomalous reflectance spectrum at a certain frequency (determined by the spacer thickness), specifically for the proposed structure, and the resonant frequency is 0.865 THz.

4. Conclusion

In this paper, a reflection-type terahertz EIT metamaterial is proposed and characterized experimentally and numerically. An electromagnetically induced reflection peak is observed between two reflection valleys from the proposed structure. The mechanism of this reflection-type terahertz EIT metamaterial is investigated by using the multiple-reflection interference theory. The results show that the reflection characteristics originate from the EIT which is generated at the metasurface and reshaped by a Fabry-Perot cavity analogue between the metasurface and the ground plane. The results of this paper provide a new type of EIT structure which may be used in many fields such as slow light effect and THz nonlinear effect.

References

[1] Harris S E 1997 *Phys. Today* **50** 36
[2] Zhang H J, Guo H J, Sun H, Li J P and Yin B Y 2013 *Chin. Phys. B* **22** 104208
[3] Zhang S, Genov D A, Wang Y, Liu M and Zhang X 2008 *Phys. Rev. Lett.* **101** 047401
[4] Papasimakis N, Fedotov V A, Zheludev N I and Prosvirnin S L 2008 *Phys. Rev. Lett.* **101** 253903
[5] Singh R, Rockstuh C, Lederer F and Zhang W L 2009 *Phys. Rev. B* **79** 085111
[6] Tassin P, Zhang L, Koschny T, Economou E N and Soukoulis C M 2009 *Phys. Rev. Lett.* **102** 053901
[7] Liu N, Langguth L, Weiss T, K¨astel J, Fleischhauer M, Pfau T and Giessen H 2009 *Nat. Mater.* **8** 758
[8] Chiam S Y, Singh R, Rockstuhl C Lederer F, Zhang W L and Bettiol A A 2009 *Phys. Rev. B* **80** 153103
[9] Li Z Y, Ma Y F, Huang R, Singh R, Gu J Q, Tian Z, Han J G and Zhang W L 2011 *Opt. Express* **19** 8912
[10] Ma Y F Li Z Y, Yang Y M, Huang R, Singh R, Zhang S, Gu J Q, Tian Z, Han J G and Zhang W L 2011 *Opt. Mater. Express* **1** 391
[11] Papasimakis N, Fu Y H, Fedotov V A, Prosvirnin S L, Tsai D P and Zheludev N I 2009 *Appl. Phys. Lett.* **94** 200902
[12] Yannopapas V, Paspalakis E and Vitanov N V 2009 *Phys. Rev. B* **80** 035104
[13] Kekatpure R D, Barnard E S, Cai W and Brongersma M L 2010 *Phys. Rev. Lett.* **104** 243902
[14] Bian C L, Zhu J, Lu J W, Yan J L, Chen L Q, Wang Z B, Ou Z Y and Zhang W P 2013 *Acta Phys. Sin.* **62** 174207 (in Chinese)
[15] Singh R, Al-Naib I A I, Yang Y P., Chowdhury D R, Cao W, Rockstuhl C, Ozaki T, Morandotti R and Zhang W L 2011 *Appl. Phys. Lett.* **99** 201107
[16] Gu J Q, Singh R, Liu X J, Zhang X Q, Ma Y F, Zhang S, Maier S A, Tian Z, Azad A K, Chen H T, Taylor A J, Han J G and Zhang W L 2012 *Nat. Commun.* **3** 1151
[17] Zhu Z H, Yang X, Gu J Q, Jiang J, Yue W S, Tian Z, Tonouchi M, Han J G and Zhang W L 2013 *Nanotechnology* **24** 214003
[18] Zhang X Q, Li Q, Cao W, Gu J Q, Singh R, Tian Z, Han J G and Zhang W L 2013 *IEEE J. Sel. Top. Quant.* **19** 1
[19] Dong Z G, Li J Q, Shao J, Yu X Q, Wang Y K and Zhai Y 2013 *Chin. Phys. B* **22** 044209
[20] Shen X P, Yang Y Zang Y Z, Gu J Q, Han J G, Zhang W L and Cui T J 2012 *Appl. Phys. Lett.* **101** 154102
[21] Chen H T 2012 *Opt. Express* **20** 7165